

Published in final edited form as:

*J Am Chem Soc.* 2012 July 18; 134(28): 11474–11480. doi:10.1021/ja3011379.

## Variations in Binding Among Several Agonists at Two Stoichiometries of the Neuronal, $\alpha 4\beta 2$ Nicotinic Receptor

Ximena Da Silva Tavares<sup>†</sup>, Angela P. Blum<sup>†</sup>, Darren T. Nakamura<sup>†</sup>, Nyssa L. Puskar<sup>†</sup>, Jai A. P. Shanata<sup>†</sup>, Henry A. Lester<sup>‡</sup>, and Dennis A. Dougherty<sup>†</sup>

<sup>†</sup>Division of Chemistry and Chemical Engineering, California Institute of Technology, Pasadena, CA 91125 USA

<sup>‡</sup>Division of Biology, California Institute of Technology, Pasadena, CA 91125 USA

### Abstract

Drug-receptor binding interactions of four agonists – ACh, nicotine, and the smoking cessation compounds varenicline (Chantix®) and cytisine (Tabex®) – have been evaluated at both the 2:3 and 3:2 stoichiometries of the  $\alpha 4\beta 2$  nicotinic acetylcholine receptor (nAChR). Previous studies have established that unnatural amino acid mutagenesis can probe three key binding interactions at the nAChR: a cation- $\pi$  interaction, and two hydrogen bonding interactions to the protein backbone of the receptor. We find that all drugs make a cation- $\pi$  interaction to TrpB of the receptor. All drugs except ACh, which lacks an N<sup>+</sup>H group, make a hydrogen bond to a backbone carbonyl, and ACh and nicotine behave similarly in acting as a hydrogen bond acceptor. However, varenicline is not a hydrogen bond acceptor to the backbone NH that interacts strongly with the other three compounds considered. In addition, we see interesting variations in hydrogen bonding interactions with cytisine that provide a rationalization for the stoichiometry selectivity seen with this compound.

### Introduction

Nicotinic acetylcholine receptors (nAChR) are pentameric ligand-gated ion channels of the central and peripheral nervous systems that are activated by the neurotransmitter acetylcholine and by nicotine and structurally related compounds <sup>1-3</sup>. These receptors have been implicated in various processes related to cognitive function, learning and memory, arousal, reward, motor control, appetite control, and analgesia <sup>4</sup>. As such, they represent therapeutic targets for the treatment of pain, epilepsy, Alzheimer's disease, Parkinson's disease, Tourette's syndrome, schizophrenia, anxiety, depression, and smoking cessation <sup>4,5</sup>.

Humans have 16 genes that code for 16 subunits that arrange as pentamers to form many different subtypes of nAChRs <sup>6</sup>. However, one particular form, termed  $\alpha 4\beta 2$ , plays an especially prominent role in nicotine addiction. This has been established by a number of pharmacological studies and by extensive evaluations of knockout mice <sup>7-9</sup>. The  $\alpha 4\beta 2$  receptor can assemble into two different stoichiometries with distinct pharmacologies <sup>10,11</sup>: ( $\alpha 4$ )<sub>2</sub>( $\beta 2$ )<sub>3</sub> and ( $\alpha 4$ )<sub>3</sub>( $\beta 2$ )<sub>2</sub>, herein referred to as A2B3 and A3B2, respectively. The A2B3

Correspondence to: Dennis A. Dougherty.

**Corresponding Author** dadougherty@caltech.edu.

**Present Addresses** J.A.P.S. : Chemistry Department, Loyola University, New Orleans, LA 70118

#### ASSOCIATED CONTENT

**Supporting Information.** Representative traces and dose-response curves; fluorination plots; and all EC<sub>50</sub> data. This material is available free of charge via the Internet at <http://pubs.acs.org>.

stoichiometry is the higher affinity form and is upregulated in response to chronic exposure to nicotine<sup>8,10</sup>, indicating that it likely plays the more prominent role in nicotine addiction.

The essential nicotinic pharmacophore – a cationic N and a hydrogen bond acceptor separated by an appropriate distance – has been established for some time<sup>12-14</sup>. In recent years, the pharmacophore has been expanded to include the pyrrolidine N<sup>+</sup>H of nicotine and similar structures as a hydrogen bond donor. Based on structural studies of the acetylcholine binding protein (AChBP)<sup>15</sup>, a useful model for the agonist binding site of nAChRs, and advanced structure-function studies, a binding model for nicotine has been developed for the  $\alpha 4\beta 2$  receptor (Figure 1). A cation- $\pi$  interaction forms between the positive charge of the drug and the highly conserved Trp154<sup>16</sup>, termed TrpB in a standard model. In addition, the N<sup>+</sup>H of the drug acts as a hydrogen bond donor to the backbone carbonyl of TrpB. Generally, drugs that have been developed to target the nAChRs have the potential to make this N<sup>+</sup>H...O=C hydrogen bond, but, of course, the endogenous agonist ACh cannot. The hydrogen bond acceptor component of the pharmacophore – the pyridine N of nicotine or the carbonyl O of ACh – makes a hydrogen bond to the backbone NH of Leu119 in the  $\beta 2$  subunit. This interaction was first revealed in a structure of AChBP with nicotine bound<sup>15</sup>, where it is mediated by a water molecule. In the actual nAChR, structure-function studies of the type described below clearly established a hydrogen bonding interaction to the backbone NH in the  $\alpha 4\beta 2$  nAChR, but did not distinguish whether the water molecule is or is not present. In the binding model of Figure 1, we have not shown the water, with the understanding that it may be important in some or all nAChRs. An additional water-mediated hydrogen bonding interaction to the backbone carbonyl corresponding to Asn107 in the  $\beta 2$  subunit is also evident in the AChBP structure, but it has not been established to be important in nAChRs. Note the interfacial nature of the agonist binding site: TrpB is in the  $\alpha$  subunit while the Leu119 backbone NH comes from the  $\beta$  subunit.

In recent work from our labs, the binding model of Figure 1 has been established to be viable for both ACh and nicotine in the A2B3 stoichiometry of the  $\alpha 4\beta 2$  receptor<sup>16</sup>. In the present work we address two key questions. First, we evaluate whether two established smoking cessation compounds fit the binding model (Figure 2A). Varenicline (marketed as Chantix® in the U.S.) was designed to target  $\alpha 4\beta 2$  receptors, and was approved for use in smoking cessation in 2006<sup>17,18</sup>. Cytisine<sup>19,20</sup> is a naturally occurring alkaloid that served as a lead compound for the development of varenicline<sup>17,18</sup>. It has been used for decades for smoking cessation and is marketed as Tabex®. Second, we probe the differential pharmacologies of the A2B3 and A3B2 stoichiometries of the  $\alpha 4\beta 2$  receptor, to determine whether the binding interactions of Figure 1 are responsible for the differences. We have applied unnatural amino acid mutagenesis to evaluate four compounds – ACh, nicotine, varenicline, and cytisine – at both the A2B3 and A3B2  $\alpha 4\beta 2$  receptors. We find many similarities, and some key differences, in the binding behaviors of these prototype drugs.

## Results

### Strategy and Methodological Issues

Unnatural amino acids were incorporated into  $\alpha 4\beta 2$  receptors using previously described nonsense suppression methodology and heterologous expression in *Xenopus laevis* oocytes<sup>21,22</sup>. Receptor function was evaluated by electrophysiology. A known Leu to Ala mutation in the M2 transmembrane helix of the  $\alpha 4$  subunit (referred to as L9'A, where 9' denotes the ninth amino acid from the cytoplasmic end of the transmembrane helix) was introduced to improve receptor expression, while maintaining pharmacological selectivity of the receptor<sup>16,23</sup>. Mutations of this type also increase receptor sensitivity to agonists, and they do so in an additive manner. Thus, in the present study, agonists acting at A3B2 receptors, with three L9'A mutations, generally show greater potency than at A2B3

receptors, which have two L9'A mutations, even though the A2B3 stoichiometry is intrinsically the high potency form.

We have previously described unnatural amino acid mutagenesis studies of the A2B3  $\alpha 4\beta 2$  receptor<sup>16</sup>, but this is the first study investigating the A3B2 form. Nonsense suppression at A3B2 receptors was challenging, due to the fact that expression of  $\alpha 4\beta 2$  in *Xenopus laevis* oocytes is inherently biased toward A2B3 receptors. For example, a 1:1  $\alpha 4$  to  $\beta 2$  mRNA injection ratio produces exclusively A2B3 receptors. The challenge of expressing A3B2 receptors was amplified when unnatural amino acids were incorporated into the  $\alpha 4$  subunit, because of the consistently lower expression levels seen for subunits incorporating unnatural amino acids by nonsense suppression. Several strategies were employed to overcome these difficulties. In order to obtain an essentially pure population of A3B2, an  $\alpha 4:\beta 2$  mRNA injection ratio at or above 100:1 was necessary. We also injected larger than usual amounts of mRNA (~100-150 ng total per oocyte, compared to the ~25 ng used in typical suppression experiments) and amino-acylated tRNA (up to 125 ng total per oocyte), and employed longer incubation times (48 – 72 h) as necessary. In especially challenging cases, we included a second injection of mRNA and tRNA 24 hrs after the initial injection, and allowed the injected oocytes to incubate at room temperature for 2-3 hours prior to electrophysiological recording. In all studies, the stoichiometry ultimately produced was verified by the previously described voltage jump protocol<sup>16</sup>, which distinguishes the two stoichiometries.

Studies of cytosine presented additional challenges. This drug is generally found to be inactive at the A2B3  $\alpha 4\beta 2$  receptor<sup>24</sup>, essentially acting as a competitive antagonist. In our hands, we find cytosine does activate the A2B3 receptor, but with very low efficacy (~3% relative to acetylcholine), compared to the 50% relative efficacy seen for the A3B2 receptor. Our ability to observe currents for the A2B3 form likely results from our incorporation of the L9'A mutation in the  $\alpha 4$  subunit. Given cytosine's low efficacy at the A2B3 stoichiometry, we used similar strategies to the ones used to study A3B2 to obtain meaningful dose-response curves for this drug-receptor combination.

We have well-established strategies for evaluating each component of the binding model of Figure 1. The existence of a cation- $\pi$  interaction has been established in a number of receptors, channels, and other proteins by successively fluorinating the aromatic amino acid of interest (Figure 2B)<sup>25,26</sup>. Fluorine substitution diminishes the cation- $\pi$  binding ability of an aromatic ring, and does so in an additive way. A correlation between the measured potency and the cation- $\pi$  binding ability of the ring establishes the existence of a cation- $\pi$  interaction.

To probe hydrogen bonding interactions to the protein backbone, we replace the appropriate amino acid with its  $\alpha$ -hydroxy analogue (Figure 2C). This converts the backbone amide to an ester, with predictable consequences. In the case of the hydrogen bond donor interaction to the carbonyl of TrpB, we replace the *i+1* residue, Thr155, with its  $\alpha$ -hydroxy analogue, Tah (threonine,  $\alpha$ -hydroxy)<sup>16,27</sup>. This attenuates the hydrogen bond-accepting ability of the backbone carbonyl, as it is an ester carbonyl rather than an amide carbonyl. To probe the hydrogen bond acceptor interaction, Leu119 of the  $\beta 2$  subunit is replaced by Lah (leucine,  $\alpha$ -hydroxy)<sup>12</sup>. This removes the backbone NH that participates in the hydrogen bond. For both strategies, we and others have seen significant impacts for mutations of this sort when a functionally significant hydrogen bond is involved<sup>28-30</sup>.

For both hydrogen bonding interactions, simply seeing an impact on receptor function from  $\alpha$ -hydroxy acid incorporation does not establish the existence of the hydrogen bond; some other aspect of receptor function could be perturbed by the mutation. At both sites, however,

we have control experiments that strongly support the hydrogen bonding model. For the hydrogen bond donor interaction, we have shown that activation by ACh is not perturbed by the backbone mutation in the A2B3 receptor. This establishes that the backbone mutation has not generically altered receptor function, and that it is indeed the N<sup>+</sup>H of the agonist that is responding to the mutation. For the hydrogen bond acceptor interaction, previous studies of nicotine at the A2B3 receptor <sup>12</sup> used a pharmacological approach to probe the hydrogen bonding interaction. The nicotine analogue S-MPP (Figure 2A) lacks the pyridine N of nicotine and so cannot participate in the backbone hydrogen bond. It responded to the backbone mutation in the A2B3 receptor very differently from nicotine, and mutant cycle analysis clearly linked the backbone NH of Leu119 to the pyridine N of nicotine. We apply the same strategy to the A3B2 form here.

The primary metric we use to evaluate receptor function is EC<sub>50</sub>, the effective concentration of agonist needed to induce half-maximal response. This is a measure of agonist potency, the concentration of drug required to produce an effect at the receptor. Since we are interested in variations in the pharmacologies of agonists, EC<sub>50</sub> is an appropriate measure for comparison. The actual process of activating a receptor such as the nAChR is complex, involving multiple equilibria reflecting drug binding to/coming off the receptor, conformational changes of the protein, and “gating” equilibria between the open and closed states of the channel. The gating process gives rise to a second metric, the efficacy of an agonist. Efficacy is a measure of the maximal response that an agonist can produce, reported here as a ratio to the response evoked by ACh. ACh is assumed to be a full agonist, producing a maximal receptor response. Other drugs may be partial agonists, producing a response that is a fraction of that produced by ACh, even at saturating concentrations. Generally, maximal potency is desirable; less drug is required to achieve a positive outcome. Maximal efficacy, however, may not always be desired. In fact, varenicline, probed here, was explicitly developed to be a partial agonist at  $\alpha 4\beta 2$ , seeking to diminish the effects of nicotine without severe craving/withdrawal symptoms<sup>18</sup>.

In studies such as these, it is typical to acknowledge the ambiguity that a change in EC<sub>50</sub> could reflect a change in “binding” or a change in “gating”. In the present study, we are probing a cation- $\pi$  interaction and two hydrogen bonds – these are unambiguously *binding* interactions. Structural models and the very subtle nature of the mutations we introduce make it clear that we are perturbing a binding interaction between the drug and the receptor. A shift in EC<sub>50</sub> indicates that the interaction probed is strengthened (or weakened) in one or more of the equilibria that contribute to EC<sub>50</sub>. A simple case would be the formation of a key hydrogen bond in the drug binding step. However, it could be that the gating equilibrium is perturbed, even if the mutation is quite remote to the region of the receptor thought to contain the channel gate. This would mean that the drug binds more tightly to the open state than to the closed (or vice versa). Either way, we are probing a binding interaction between the drug and the receptor. Certainly, there is value in knowing which step of the overall equilibrium is most sensitive to the interaction being probed. Single-channel studies with the patch clamp can provide such information, and we have used this approach in the past to further characterize unnatural amino acid mutations we have made. In the present work we present over 60 EC<sub>50</sub> values obtained from multiple dose-response curves (Supporting Information). It is not feasible to perform single-channel studies on every combination of drug and mutation considered here. More importantly, for studies of comparative pharmacology, EC<sub>50</sub> is arguably the most appropriate measure of receptor function.

### The cation- $\pi$ interaction

Previously we have shown that both ACh and nicotine make a cation- $\pi$  interaction to TrpB (Trp154) in the A2B3  $\alpha 4\beta 2$  receptor <sup>16</sup>. In the present work, we establish comparable

cation- $\pi$  interactions for varenicline and cytosine at A2B3 and for all four agonists at the A3B2 receptor. Plots of cation- $\pi$  binding ability (which correlates with the degree of fluorination) vs. log EC<sub>50</sub> are linear in all cases (Supporting Information).

We have previously argued that the magnitude of the perturbation to EC<sub>50</sub> induced by fluorination can be taken as an indicator of the relative strength of a cation- $\pi$  interaction<sup>31</sup>. In Table 1 we characterize the strength of a cation- $\pi$  interaction by the ratio of EC<sub>50</sub> values for the F<sub>4</sub>-Trp mutant vs. the wild type. The F<sub>4</sub>-Trp residue represents a side chain in which the electrostatic component of the cation- $\pi$  interaction has been completely removed, but other features of the residue are essentially intact (Figure 3). As shown in Table 1, all drug-receptor pairings reported here show a significant “cation- $\pi$  ratio”, thus establishing a common anchor point for the binding of all drugs considered here to both receptors.

### The hydrogen bond donor

All the agonists that possess an N<sup>+</sup>H moiety are significantly impacted by the Thr155Tah mutation in both stoichiometries, suggesting the hydrogen bond donor interaction to the backbone carbonyl of TrpB is significant. ACh is not impacted by this mutation, as expected. To facilitate comparison, we have again expressed variations as a ratio of EC<sub>50</sub> values, comparing the receptor with Tah at residue 155 to the wild type Thr (Table 1). All agonists except ACh show an EC<sub>50</sub> ratio significantly greater than 1, with only modest variations in magnitude.

### The hydrogen bond acceptor

In previous studies of the A2B3 receptor<sup>12</sup>, we showed that ACh and nicotine respond equivalently to the  $\beta$ 2 Leu119Lah mutation, with a moderate rise in EC<sub>50</sub>. Importantly, we showed that analogs that lack the hydrogen bond acceptor moiety – SMPP for nicotine (Figure 2) and choline for ACh – responded quite differently to the  $\beta$ 2 Leu119Lah mutation. This established that it is, indeed, the pyridine N of nicotine and the carbonyl O of ACh that interact with the backbone NH. We now report parallel results for ACh and nicotine in the A3B2 receptor. Again, expressing our results as a ratio of EC<sub>50</sub> values for backbone mutant vs. wild type receptors, both compounds show moderate increases in EC<sub>50</sub> in response to the backbone ester in both receptor stoichiometries (Table 1). However, choline is not impacted by the mutation, and S-MPP is actually *gain of function* in response to the backbone mutation in the A3B2 receptor (Supporting Information). A similar result was seen for S-MPP in the A2B3 receptor<sup>12</sup>.

The results for varenicline are surprising and stand in contrast to those for ACh and nicotine. With only a 2-fold shift in A2B3 and no meaningful shift in A3B2, it would appear that there is no functionally significant hydrogen bond acceptor interaction between a quinoxaline N of varenicline and the backbone NH of  $\beta$ 2 Leu119 in the  $\alpha$ 4 $\beta$ 2 receptor.

Cytosine also produces intriguing results for the hydrogen bond acceptor interaction. A remarkable 62-fold shift is seen for this subtle mutation in the A2B3 receptor. A much smaller effect is seen in the A3B2 receptor, although it is still larger than seen for any other drug-receptor combination.

## Discussion

From a combination of structural and functional studies, strong evidence has emerged for an agonist binding model at the nAChR that consists of three distinct binding interactions: a cation- $\pi$  interaction, a hydrogen bond donor interaction to a backbone carbonyl, and a hydrogen bond acceptor interaction to a backbone NH. In the present work we have



evaluated these three interactions for four different agonists at two stoichiometries of the  $\alpha 4\beta 2$  receptor.

A cation- $\pi$  interaction to TrpB (Trp154) has been found in both stoichiometries of the  $\alpha 4\beta 2$  receptor for all compounds studied here: ACh, nicotine, varenicline, and cytosine. The data of Table 1 suggest mostly modest variations, with perhaps two meaningful differences. At both stoichiometries, ACh shows the strongest cation- $\pi$  interaction of the four drugs. Note that intrinsically (i.e., in the gas phase) a quaternary ammonium cation as in ACh makes a weaker cation- $\pi$  interaction than a protonated amine<sup>32,33</sup>. It would appear that the nAChR evolved to optimize this interaction for its natural agonist, ACh. Also, for both ACh and nicotine, the A3B2 stoichiometry produces a stronger cation- $\pi$  interaction than the A2B3. No meaningful differences are seen for varenicline or cytosine.

We have argued that F<sub>4</sub>-Trp represents a side chain for which the electrostatic component of the cation- $\pi$  interaction has been completely removed, while other secondary effects such as dispersion forces and induced dipole interactions remain. The EC<sub>50</sub> ratios of Table 1 thus provide an estimate of the magnitude of this effect. For the largest interaction – ACh in A3B2 – the ratio of 540 corresponds to a  $\Delta G^\circ$  value of 3.7 kcal/mol. This is consistent with other estimations of the cation- $\pi$  interaction in protein systems<sup>34-36</sup>.

The cation- $\pi$  interaction is a universal feature of ACh binding sites, but some variations have been seen. For example, a cation- $\pi$  interaction is seen for ACh but *not* for nicotine in the muscle-type nAChR (( $\alpha_1$ )<sub>2</sub>) $\beta 1\gamma\delta$ )<sup>16,31</sup>, a key feature in distinguishing peripheral vs. central nervous system effects of nicotine. In the muscle-type nAChR, the much more potent nicotine analogue epibatidine does show a cation- $\pi$  interaction to TrpB<sup>27</sup>. In the  $\alpha 4\beta 4$  nAChR (A2B3 stoichiometry), both ACh and nicotine make a cation- $\pi$  interaction to TrpB<sup>37</sup>. However, in the homopentameric  $\alpha 7$  nAChR, the cation- $\pi$  site moves to an alternative aromatic residue in the agonist binding site<sup>37</sup>. Similar results are seen for other members of Cys-loop (pentameric) superfamily of neurotransmitter-gated ion channels. In the 5-HT<sub>3</sub> (serotonin) receptor<sup>31</sup>, the glycine receptor<sup>38</sup>, and the GABA<sub>A</sub> and GABA<sub>C</sub> receptors<sup>39,40</sup>, the agonist makes a cation- $\pi$  interaction to an aromatic residue at the agonist binding site. The analogue to TrpB is the most common cation- $\pi$  site, but some variation is seen across the family<sup>25</sup>. For the drug-receptor combinations probed here, however, all cation- $\pi$  interactions are to TrpB.

Two hydrogen bonding interactions contribute to agonist binding, and we have referred to them as the hydrogen bond donor and the hydrogen bond acceptor of the drug (Figure 1). Of course, ACh cannot participate in the hydrogen bond donor interaction, but nicotine shows a strong interaction with the backbone carbonyl of TrpB. For ACh and nicotine, both stoichiometries show similar behaviors for the hydrogen bond acceptor interaction.

The two smoking cessation compounds, varenicline and cytosine, show interesting variations with regard to hydrogen bonding interactions. In discussing these compounds, we will refer to Figure 4, which shows structures and electrostatic potential surfaces for ACh, nicotine, cytosine, and varenicline.

Varenicline is similar to nicotine in its participation in the hydrogen bond donor interaction. However, varenicline is qualitatively different from all the other compounds considered with regard to the hydrogen bond acceptor interaction. With less than a 2-fold effect at the A2B3 stoichiometry and no meaningful effect at the A3B2 stoichiometry, we conclude that varenicline does not make a functionally important hydrogen bond to the backbone NH of Leu119 in the  $\beta 2$  subunit. Figure 4 provides a rationalization. By visual inspection, and from the distances shown, is it clear that the quinoxaline nitrogens of varenicline are not well aligned with the hydrogen bond acceptor moieties of the other compounds. Thus, it may be

that the geometry of varenicline makes formation of the hydrogen bond impossible. Alternatively, the quinoxaline N is a much poorer hydrogen bond acceptor than the pyridine N of nicotine ( $pK_a$  values for pyridine and quinoxaline are 5.2 and 0.8, respectively). It may be that the protein can adjust to the geometry of varenicline, but the hydrogen bonding interaction is so weak that it does not show up in our assay.

Cytisine shows an intriguing hydrogen bonding pattern, distinct from the other agonists considered here. Recall that, more so than the other drugs, cytisine shows a strong distinction between the two stoichiometries of the  $\alpha 4\beta 2$  receptor. Generally, cytisine is considered to be inactive (an antagonist) at the A2B3 form; we are able to record  $EC_{50}$  values because of the L9'A mutations present in our system. Cytisine is however efficacious at the A3B2 form. Interestingly, cytisine also shows the greatest stoichiometry differences for both hydrogen bonding interactions (Table 1). Concerning the hydrogen bond donor interaction, cytisine shows a stronger than usual hydrogen bond in the A3B2 stoichiometry, but a weaker than usual interaction in the A2B3 stoichiometry. The effects are not large, but we feel the systems being compared are similar enough that the differences are meaningful. The pattern is reversed in the hydrogen bond acceptor site. The A2B3 stoichiometry shows a remarkable 62-fold rise in  $EC_{50}$  in response to the backbone mutation, much larger than anything we have seen previously. The A3B2 stoichiometry now shows the smaller effect, although it is still larger than what is seen with nicotine or ACh.

We propose a speculative model to rationalize these results. Recall that cytisine is efficacious at A3B2 but not at A2B3. Also, A3B2 shows a strong hydrogen bond donor interaction and a relatively weaker hydrogen bond acceptor interaction, while the reverse pattern holds for A2B3. We propose that cytisine is positioned closer to TrpB in the efficacious A3B2 stoichiometry than in the A2B3, and that a strong interaction with TrpB is required for receptor gating. By moving closer to TrpB in the A3B2 receptor, cytisine is moving further from Leu119, thus explaining the pattern of hydrogen bond strengths. Hydrogen bonding shows a fairly steep distance dependence, and so only a slight shift would be required to meaningfully strengthen/weaken a hydrogen bond. In contrast, the cation- $\pi$  interaction is much less sensitive to the distance separation between the charge and the  $\pi$  system<sup>34</sup>, and so there is no stoichiometry distinction for this interaction. As noted above, for some indications a partial agonist could be preferable to a full agonist. If validated by further studies, the present findings could suggest a strategy for tuning agonist efficacy. Maximizing the interaction with TrpB, through both the cation- $\pi$  interaction and the hydrogen bond donor interaction, should maximize efficacy, while biasing the system toward the hydrogen bond acceptor interaction could diminish efficacy.

Another aspect of cytisine's pharmacology is that the hydrogen bond acceptor interaction is stronger for *both* stoichiometries than for the any of the other drug-receptor pairs. We can rationalize this general effect with reference to the electrostatic potential plots of Figure 4. Visually, the carbonyl oxygen of cytisine presents a much stronger negative electrostatic potential than the corresponding nitrogen of nicotine. Quantitative evaluation of the electrostatic potentials at these atoms confirms the visual impression. Thus, the amide carbonyl oxygen of cytisine should be a better hydrogen bond acceptor than the pyridine nitrogen of nicotine or the ester carbonyl of ACh, completely consistent with expectations based on known hydrogen bonding propensities.

In conclusion, we have evaluated a binding model for ACh, nicotine, and two smoking cessation drugs, varenicline and cytisine, at both stoichiometries of the  $\alpha 4\beta 2$  nAChR, the receptor most associated with nicotine addiction. We find a universal cation- $\pi$  interaction, and a hydrogen bond donor interaction to a backbone carbonyl. However, we find that varenicline violates the nicotinic binding model and does not make a functionally significant

hydrogen bond acceptor interaction seen with other agonists. In addition, the differential hydrogen bonding interactions for cytosine suggest a structural model to explain the variation in efficacy seen for the two receptor stoichiometries.

## Experimental Details

### Mutagenesis and mRNA synthesis

Rat  $\alpha 4L9'A$  and  $\beta 2$  subunits were expressed in pAMV vectors. The mutations for each subunit were introduced according to the QuikChange mutagenesis protocol (Stratagene) and sequencing verified the incorporation of desired mutations. Rat  $\alpha 4L9'A$  and  $\beta 2$  mRNA were prepared from NotI linearizations of the circular expression vector pAMV, followed by *in vitro* transcription using the mMessage mMachine T7 kit (Ambion, Austin, TX).

### Ion channel expression

To express the ion channels with a wild type ligand binding site,  $\alpha 4L9'A$  mRNA was co-injected with  $\beta 2$  mRNA at various ratios to obtain desired receptor stoichiometry. Specifically, 20:1  $\alpha 4L9'A$ : $\beta 2$  ratio for A3B2 and 1:3 for A2B3. Total mRNA amount for microinjection was 10-50 ng/cell in a total volume of 75 nL. Stage V-VI *Xenopus laevis* oocytes were microinjected and incubated at 18°C for 24-48 h in ND96 buffer (96 mM NaCl, 2 mM KCl, 1 mM MgCl<sub>2</sub>, 2 mM CaCl<sub>2</sub>, and 5 mM HEPES, pH 7.5) with 0.005% (w/v) gentamycin and 2% (v/v) horse serum.

### Unnatural amino acid / $\alpha$ -hydroxy acid incorporation

Nitroveratryloxycarbonyl (NVOC) protected cyanomethyl ester forms of unnatural amino acids and  $\alpha$ -hydroxythreonine cyanomethyl ester were synthesized, coupled to the dinucleotide dCA, and enzymatically ligated to either 74-nucleotide THG73 tRNA (for  $\alpha 4W154$  and  $\alpha 4T155$  experiments) or 74-nucleotide TQOpS' tRNA (for  $\beta 2L119$  experiments) as described previously<sup>16,21</sup>. The unnatural amino acid-conjugated tRNA was deprotected by photolysis and then immediately co-injected with mRNA containing the UAG mutation (for THG73 tRNA) or the UGA mutation (TQOpS' tRNA) at the site of interest. Stage V-VI oocytes were injected with ~10-150 ng mRNA and 25-125 ng tRNA-amino acid or tRNA-hydroxy acid in a total volume of 75 nL. For unnatural amino acid incorporation into the  $\alpha 4$  subunit, a 3:1  $\alpha 4L9'A$ : $\beta 2$  mRNA injection ratio yielded A2B3 receptors and 100:1 to 150:1 ratios yielded A3B2 receptors. For unnatural amino acid incorporation into the  $\beta 2$  subunit, a 1:20  $\alpha 4L9'A$ : $\beta 2$  mRNA injection ratio yielded A2B3 receptors and a 10:1 ratio yielded A3B2 receptors. In cases where receptor expression needed to be increased, a second microinjection (double injection) of the same concentration and volume of  $\alpha 4L9'A$ : $\beta 2$  mRNA and tRNA was performed after 24 h incubation at 18 °C. Double injected oocytes were incubated for an additional 24-48 h for a total of 48-72 h. Cells were incubated in ND96 buffer, 0.005% (w/v) gentamycin and 2% (v/v) horse serum, and the solution was changed at least daily and up to every 6 hrs. The fidelity of unnatural amino acid incorporation was confirmed at each site with a "wild type recovery" experiment and "read-through/reaminoacylation" tests. In the "wild type recovery" experiment, UAG mutant mRNA was co-injected with tRNA charged with the amino acid that was present at this residue in the wild type protein. Generation of receptors that were indistinguishable from the wild type protein indicated that the residue carried by the suppressor tRNA was successfully and exclusively integrated into the protein. In a "read-through/reaminoacylation" test, the UAG mutant mRNA was introduced with (1) no tRNA, (2) tRNA THG73 that was not charged with any amino acid or (3) tRNA THG73 enzymatically ligated to the dinucleotide dCA. A lack of current in these experiments validated the reliability of the nonsense suppression experiments.



## Whole-cell electrophysiological characterizations of the channels

Oocyte recordings were performed 24 h after microinjection for wild type receptors and 48 to 72 h after microinjection for unnatural amino acids. Agonist-induced currents were recorded in two-electrode voltage clamp mode using the OpusXpress 6000A (Axon Instruments, Union City, CA) at a holding potential of  $-60$  mV. Oocytes were superfused with  $\text{Ca}^{2+}$ -free ND96 solution (96 mM NaCl, 2 mM KCl, 1 mM  $\text{MgCl}_2$ , and 5 mM HEPES, pH 7.5) at flow rates of either 0.6 or 4 mL/min during drug application and 3 mL/min during wash. For A2B3 experiments, drug application was 15 s in duration at 4 mL/min rate (1 mL total drug volume), while wash duration between each concentration was 116 s. For A3B2 experiments, drug application was 15 s in duration at 4 mL/min rate immediately followed by 105 s at 0.6 mL/min rate (2 mL total drug volume), while wash duration between each concentration was 116 s. Data were sampled at 50 Hz and filtered at 20 Hz. Acetylcholine chloride, (–)-nicotine tartrate, and (–)-cytisine were purchased from Sigma/Aldrich/RBI (St. Louis, MO). Varenicline tartrate was a generous gift from Targacept company. Agonists were prepared in sterile, distilled, deionized water for dilution in  $\text{Ca}^{2+}$ -free ND96 solution. Dose-response data were obtained for at least 6 concentrations of agonist and for a minimum of 5 oocytes originating from at least two different donor frogs. Mutants with  $I_{\text{max}}$  of at least 80 nA of current were defined as functional.  $\text{EC}_{50}$  and Hill coefficients were calculated by fitting the dose-response relation to the Hill equation. The dose-responses of individual oocytes were examined to identify outliers. All data are reported as mean  $\pm$  standard error (SE). Voltage jump experiments were used to verify the stoichiometry of the mutant and wild type receptors, as described previously.

## Supplementary Material

Refer to Web version on PubMed Central for supplementary material.

## Acknowledgments

This work was supported by the National Institutes of Health [Grants NS34407 NS11756] and by the California Tobacco-Related Disease Research Program of the University of California, Award 19XT-0102

## ABBREVIATIONS

<b>ACh</b>	acetylcholine
<b>nAChR</b>	nicotinic acetylcholine receptors
<b>AChBP</b>	acetylcholine binding protein
<b>S-MPP</b>	S-N-methyl-2-phenylpyrroline
<b>tRNA</b>	transfer RNA
<b>A2B3</b>	$(\alpha 4)_2(\beta 2)_3$
<b>A3B2</b>	$(\alpha 4)_3(\beta 2)_2$

## References

1. Corringer PJ, Le Novère N, Changeux JP. Annu Rev Pharmacol Toxicol. 2000; 40:431. [PubMed: 10836143]
2. Grutter T, Changeux JP. Trends Biochem Sci. 2001; 26:459. [PubMed: 11504610]
3. Karlin A. Nat Rev Neurosci. 2002; 3:102. [PubMed: 11836518]
4. Jensen AA, Frolund B, Lijefors T, Krogsgaard-Larsen P. Journal of Medicinal Chemistry. 2005; 48:4705. [PubMed: 16033252]

5. Gotti C, Zoli M, Clementi F. Trends in Pharmacological Sciences. 2006; 27:482. [PubMed: 16876883]
6. Millar NS, Gotti C. Neuropharmacology. 2009; 56:237. [PubMed: 18723036]
7. Mansvelder HD, Keath JR, McGehee DS. Neuron. 2002; 33:905. [PubMed: 11906697]
8. Nashmi R, Xiao C, Deshpande P, McKinney S, Grady SR, Whiteaker P, Huang Q, McClure-Begley T, Lindstrom JM, Labarca C, Collins AC, Marks MJ, Lester HA. Journal of Neuroscience. 2007; 27:8202. [PubMed: 17670967]
9. Tapper AR, McKinney SL, Nashmi R, Schwarz J, Deshpande P, Labarca C, Whiteaker P, Marks MJ, Collins AC, Lester HA. Science. 2004; 306:1029. [PubMed: 15528443]
10. Kuryatov A, Luo J, Cooper J, Lindstrom J. Molecular Pharmacology. 2005; 68:1839. [PubMed: 16183856]
11. Nelson ME, Kuryatov A, Choi CH, Zhou Y, Lindstrom J. Molecular Pharmacology. 2003; 63:332. [PubMed: 12527804]
12. Blum AP, Lester HA, Dougherty DA. Proceedings of the National Academy of Sciences of the United States of America. 2010; 107:13206. [PubMed: 20616056]
13. Glennon RA, Dukat M, Liao L. Current Topics in Medicinal Chemistry. 2004; 4:631. [PubMed: 14965299]
14. Beers WH, Reich E. Nature. 1970; 228:917. [PubMed: 4921376]
15. Celie PHN, van Rossum-Fikkert SE, van Dijk WJ, Brejc K, Smit AB, Sixma TK. Neuron. 2004; 41:907. [PubMed: 15046723]
16. Xiu XA, Puskar NL, Shanata JAP, Lester HA, Dougherty DA. Nature. 2009; 458:534. [PubMed: 19252481]
17. Coe JW, Brooks PR, Vetelino MG, Wirtz MC, Arnold EP, Huang JH, Sands SB, Davis TI, Lebel LA, Fox CB, Shrikhande A, Heym JH, Schaeffer E, Rollema H, Lu Y, Mansbach RS, Chambers LK, Rovetti CC, Schulz DW, Tingley FD, O'Neill BT. Journal of Medicinal Chemistry. 2005; 48:3474. [PubMed: 15887955]
18. Coe JW, Brooks PR, Wirtz MC, Bashore CG, Bianco KE, Vetelino MG, Arnold EP, Lebel LA, Fox CB, Tingley FD, Schulz DW, Davis TI, Sands SB, Mansbach RS, Rollema H, O'Neill BT. Bioorganic & Medicinal Chemistry Letters. 2005; 15:4889. [PubMed: 16171993]
19. Etter J-F. Archives of Internal Medicine. 2006; 166:1553. [PubMed: 16908787]
20. Etter J-F, Lukas RJ, Benowitz NL, West R, Dresler CM. Drug and Alcohol Dependence. 2008; 92:3. [PubMed: 17825502]
21. Nowak MW, Gallivan JP, Silverman SK, Labarca CG, Dougherty DA, Lester HA. Methods Enzymol. 1998; 293:504. [PubMed: 9711626]
22. Nowak MW, Kearney PC, Sampson JR, Saks ME, Labarca CG, Silverman SK, Zhong W, Thorson J, Abelson JN, Davidson N, Schultz PG, Dougherty DA, Lester HA. Science. 1995; 268:439. [PubMed: 7716551]
23. Fonck C, Cohen BN, Nashmi R, Whiteaker P, Wagenaar DA, Rodrigues-Pinguet N, Deshpande P, McKinney S, Kwok S, Munoz J, Labarca C, Collins AC, Marks MJ, Lester HA. Journal of Neuroscience. 2005; 25:11396. [PubMed: 16339034]
24. Moroni M, Zwart R, Sher E, Cassels BK, Bermudez I. Molecular Pharmacology. 2006; 70:755. [PubMed: 16720757]
25. Dougherty DA. Chem. Rev. 2008; 108:1642. [PubMed: 18447378]
26. Dougherty DA. J Org Chem. 2008; 73:3667. [PubMed: 18412391]
27. Cashin AL, Petersson EJ, Lester HA, Dougherty DA. J. Am. Chem. Soc. 2005; 127:350. [PubMed: 15631485]
28. Deechongkit S, Nguyen H, Powers ET, Dawson PE, Gruebele M, Kelly JW. Nature. 2004; 430:101. [PubMed: 15229605]
29. Koh JT, Cornish VW, Schultz PG. Biochemistry. 1997; 36:11314. [PubMed: 9298950]
30. England PM, Zhang Y, Dougherty DA, Lester HA. Cell. 1999; 96:89. [PubMed: 9989500]
31. Beene DL, Brandt GS, Zhong WG, Zacharias NM, Lester HA, Dougherty DA. Biochemistry. 2002; 41:10262. [PubMed: 12162741]

32. Deakyne CA, Meotner M. *Journal of the American Chemical Society*. 1985; 107:474.
33. Meotner M, Deakyne CA. *Journal of the American Chemical Society*. 1985; 107:469.
34. Dougherty DA. *Science*. 1996; 271:163. [PubMed: 8539615]
35. Ma JC, Dougherty DA. *Chem. Rev.* 1997; 97:1303. [PubMed: 11851453]
36. Ting AY, Shin I, Lucero C, Schultz PG. *Journal of the American Chemical Society*. 1998; 120:7135.
37. Puskar NL, Xiu XA, Lester HA, Dougherty DA. *Journal of Biological Chemistry*. 2011; 286:14618. [PubMed: 21343288]
38. Pless SA, Hanek AP, Price KL, Lynch JW, Lester HA, Dougherty DA, Lummis SCR. *Molecular Pharmacology*. 2011; 79:742. [PubMed: 21266487]
39. Lummis SCR, Beene DL, Harrison NJ, Lester HA, Dougherty DA. *Chemistry & Biology*. 2005; 12:993. [PubMed: 16183023]
40. Padgett CL, Hanek AP, Lester HA, Dougherty DA, Lummis SCR. *Journal of Neuroscience*. 2007; 27:886. [PubMed: 17251430]

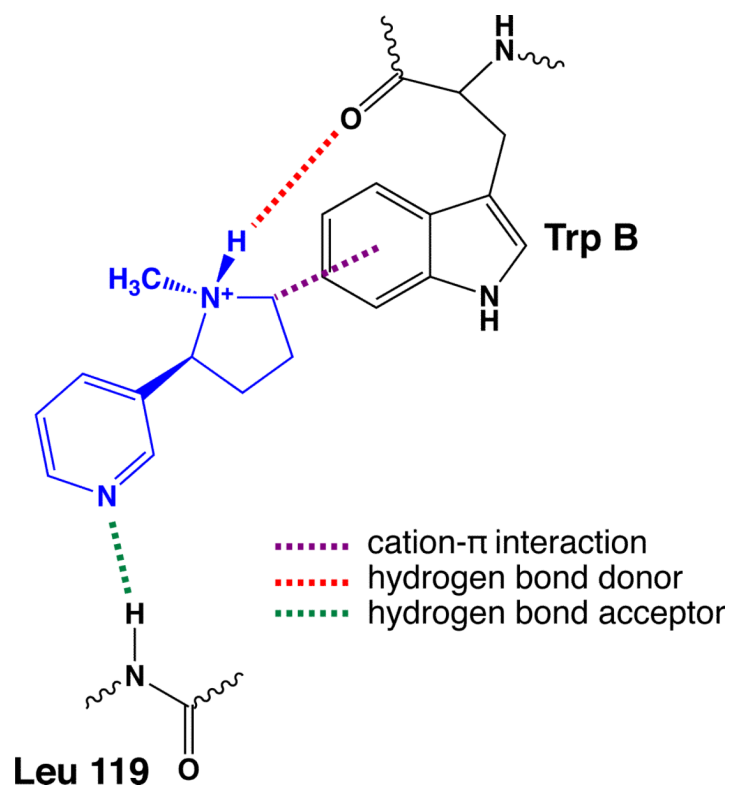


**Fig. 1.**  
The binding model for nicotine at an nAChR that is evaluated in the present work.

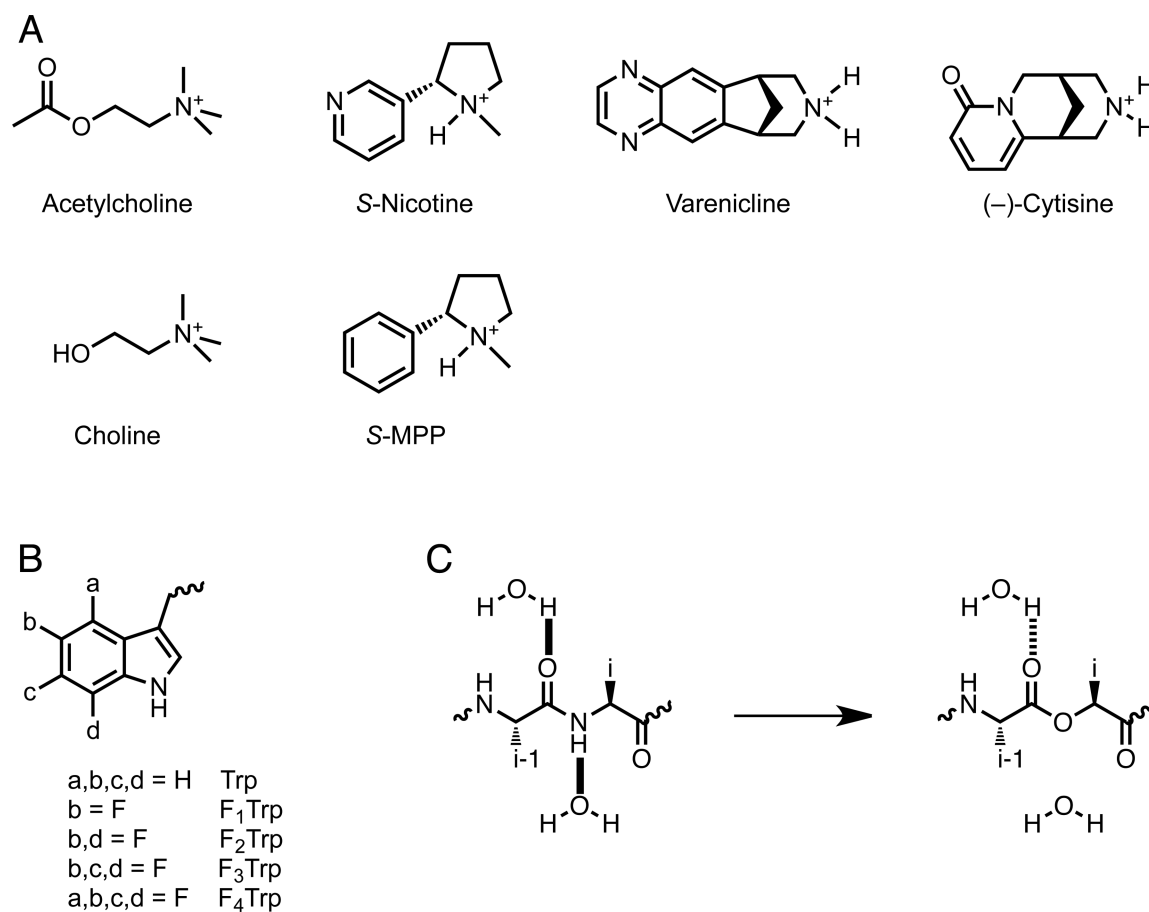


**Fig. 2.**  
 Chemical Structures. A. Agonists used in this study. B. Unnatural amino acids employed here. If not indicated, an a, b, c, or d group is H. C. Backbone ester strategy for modulating hydrogen bonds.



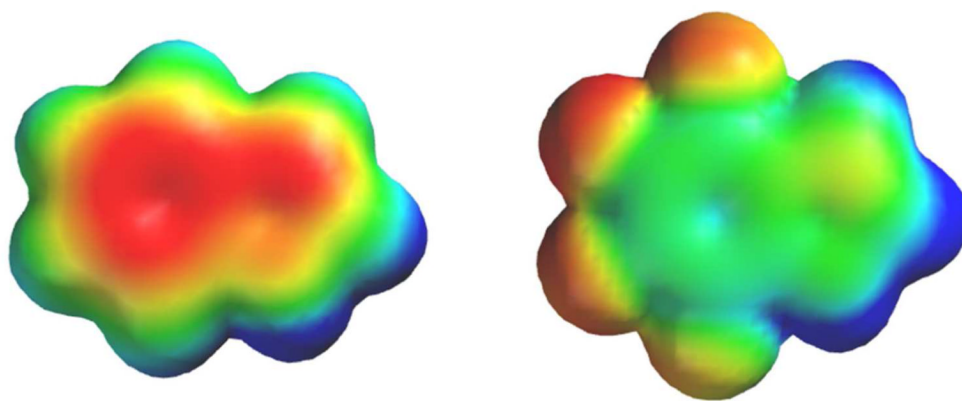


**Fig. 3.** Electrostatic potential surfaces of indole (left) and F<sub>4</sub>-indole, corresponding to the aromatic portions of the side chains of Trp and F<sub>4</sub>-Trp, respectively. Results are from HF-6-31G\*\* calculations. Electrostatic potential ranges from -25 kcal/mol (red) to +25 kcal/mol (blue), so that green represents ~0 electrostatic potential.

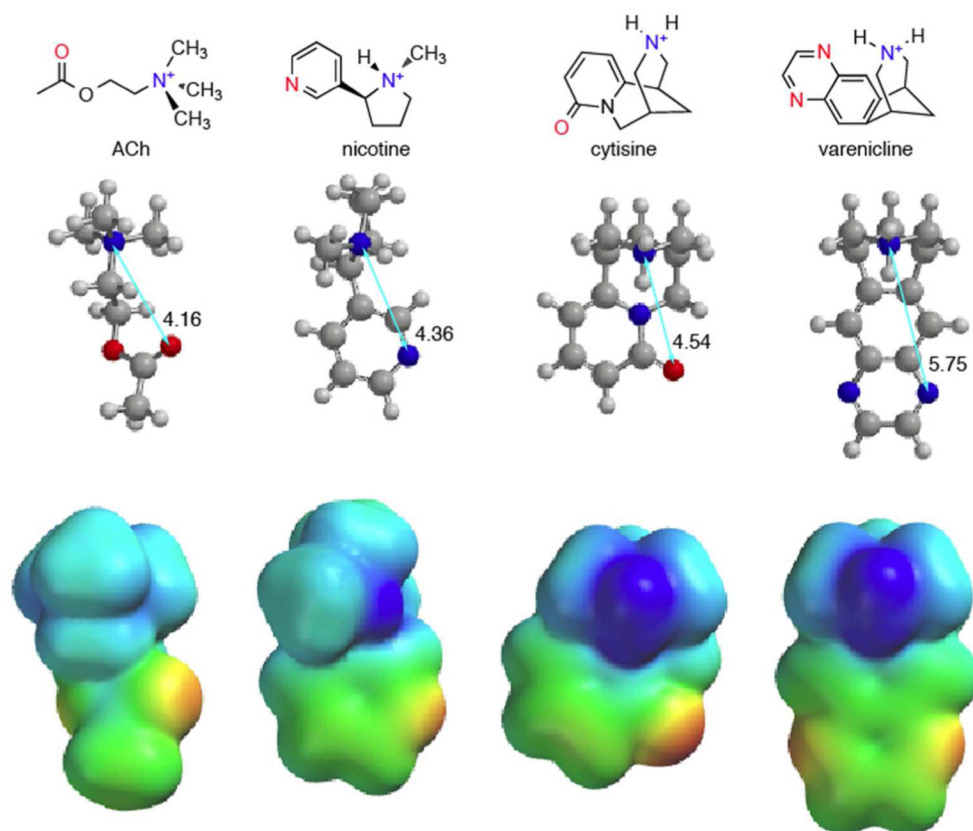


**Fig. 4.** Structures and electrostatic potential surfaces for the agonists considered here. Results are from HF-3-21G\* calculations. Electrostatic potential ranges from -4.8 kcal/mol (red) to +143 kcal/mol (blue). As such, unlike in Figure 3, green does not represent ~0 electrostatic potential. As all these molecules are cations, the surfaces are positive over their entirety, except for a small negative electrostatic potential at the carbonyl oxygen of cytosine.

Table 1

Evaluation of Binding Interactions in the  $\alpha 4\beta 2$  receptor.

		wild type EC <sub>50</sub> ( $\mu$ M) <sup>a</sup>	relative efficacy <sup>b</sup>	Cation- $\pi$ interaction <sup>c</sup>	N <sup>+</sup> -H...O=C (donor) <sup>d</sup>	N-H...N(O) (acceptor) <sup>e</sup>
ACh	A2B3	4.0	[1.0]	69 <sup>f</sup>	1.1 <sup>f</sup>	6.8 <sup>g</sup>
	A3B2	87	[1.0]	540	1.1	8.5
Nicotine	A2B3	0.76	0.3 (0.3)	53 <sup>f</sup>	19 <sup>f</sup>	6.7 <sup>g</sup>
	A3B2	38	0.6 (0.6)	130	19	5.6
Varenicline	A2B3	0.027	0.1	20	14	1.8
	A3B2	3.6	0.3	16	19	1.1
Cytisine	A2B3	0.066	0.03 (0)	31	8.8	62
	A3B2	15	0.5 (0.2)	30	27	14

<sup>a</sup>Values are corrected for the effects of  $\alpha 4$  L9'A mutation according to the procedure of Moroni et al.<sup>24</sup> As such, these are EC<sub>50</sub> for true wild type receptors. Measured EC<sub>50</sub> values are provided in Supporting Information.

<sup>b</sup>Defined as the ratio  $I_{max}$  of agonist/  $I_{max}$  of ACh. Numbers in parentheses represent efficacies for receptors that do not contain the L9'A mutation, as reported by Moroni, et al.<sup>24</sup>

<sup>c</sup>Ratio of EC<sub>50</sub> values for E4-Trp/Trp at position 154 in  $\alpha 4$ .

<sup>d</sup>Ratio of EC<sub>50</sub> values for Tah/Thr at position 155 in  $\alpha 4$ .

<sup>e</sup>Ratio of EC<sub>50</sub> values for Lah/Leu at position 119 in  $\beta 2$ .

<sup>f</sup>Previously reported in<sup>16</sup>.

<sup>g</sup>Previously reported in<sup>12</sup>.